Towards a Natural Motion Generator: a Pipeline to Control a Humanoid based on Motion Data

Sungjoon Choi and Joohyung Kim

Abstract— **Imitation of the upper body motions of human demonstrators or animation characters to human-shaped robots is studied in this paper. We present a pipeline for motion retargeting by transferring the joints of interest (JOI) of source motions to the target humanoid robot. To this end, we deploy an optimization-based motion retargeting method utilizing link length modifications of the source skeleton and a task (Cartesian) space fine-tuning of JOI motion descriptors. To evaluate the effectiveness of the proposed pipeline, we use two different 3-D motion datasets from three human demonstrators and an Ogre animation character, *Bork*, and successfully transfer the motions to four different humanoid robots: DARwIn-OP, COmpliant HuMANoid Platform (COMAN), THORMANG, and Atlas. Furthermore, COMAN and THORMANG are actually controlled to show that the proposed method can be deployed to physical robots.**

I. Introduction

Since the first animatronic human figure of Abraham Lincoln made its famous sit-to-stand motion in 1964, the Walt Disney company has been developing a number of human-shaped animatronics for Disney parks. Nowadays, humanoid robots are common in many of amusement parks, as well as in smaller scale attractions, such as museums and theme restaurants. Robotics researchers and artists in the entertainment field have been collaborating together to implement realistic shapes and natural motions of notable people in history or characters in movies and animations. Advancement in measurements and graphics technologies, including a motion capture (MoCap) system, have contributed much to the motion generation for the entertainment humanoid robots. Still, however, a natural motion generation for a humanoid robot requires a number of tedious and time-consuming manual processes. In this regards, we need easier and automated methods to handle a large number motion databases for robots with different morphologies [1].

In this paper, we propose an efficient pipeline to generate expressive movements of a humanoid robot using 3-D motion data acquired from human demonstrators or animation characters. While there are a number of different methods for generating motions for a humanoid robot, we cast this problem as a motion retargeting problem where the goal is to find a mapping between the source motion data and a target robot hardware. This motion retargeting often requires a considerable amount of domain knowledge regarding the robot hardware as well as and a manual design of retargeting processes. For example, a real-time motion retargeting method in [2] manually designed a mapping between the joint angles of a source human skeleton acquired from a Xsens MoCap system and the target iCub humanoid robot.

Here, we mainly focus on simple and straightforward deployment of upper-body motions to human-like robots to minimize the tedious manual design processes. To this end, we present a global optimization-based motion retargeting method that can be applied with the minimal domain information on both motion data and the kinematic structure of a robot. The only manual process is to specify the joints of interest (JOI) of both the source MoCap skeleton and the target humanoid robot. As a result, we successfully transfer 36 different motions collecte from human demonstrator and an animation character to four humanoid robots whose sizes and morphologies vary significantly.

The main contribution of this paper is twofold. First, we present an effective parametrization of motion transfer considering both the kinematic structure of 3-D motion data and the task-space fine-tuning. Then we present a cost function for assessing the quality of the retargeting which allows us to use a global optimization method that considers the similarities between the source and target motions as well as physical constraints of a humanoid robot such as maximum joint limits and workspaces of joints, e.g., hands and elbows.

The structure of this paper is organized as follows: In Section II, we summarize existing motion retargeting methods in both robotics and computer graphics domains. A brief introduction to a global optimization method that we use for motion retargeting is shown in Section III. The proposed optimization-based motion retargeting method and results are illustrated in Section IV and Section V, respectively.

II. Related Work

A motion retargeting problem was originally presented in the computer graphics field where the problem was to simply transfer the motions of one character to the another with the identical kinematic structure but different link lengths while preserving the qualities of the original motion [3]. However, following studies [4]–[6] considered transferring motions to fairly different kinematic structures. [4] presented style-based inverse kinematics (IKs) using a Gaussian process latent variable model (GPLVM) [7] that can provide the most likely positions given algebraic constraints such as target points. Later work from [5] proposed a method to animate characters whose topologies are significantly different from humans such as a lamp or a penguin also using a GPLVM. The main idea was to optimize a shared latent space between

Sungjoon Choi and Joohyung Kim are with Disney Research, 521 Circle Seven Drive, Glendale, CA 91201, USA. {sungjoon.choi, joohyung.kim}@disneyresearch.com

human and character motion spaces. However, this method requires enough motions of both source MoCap data and the target animation characters which is hard to achieve when using real robot hardwares. Convenient and flexible generation of motions of humanoids was studied in [8] by presenting an interactive inverse kinematics technique called *pin and drag*. It allows animators to generate a natural motion of a humanoid by simply dragging a link.

DeepMimic was presented in [9] by formulating a motion imitation problem as a reinforcement learning problem where motion retargeting problems are also handled. The main idea is to use the motion similarity between the source and target motions as a reward signal to train an imitating policy of a target platform. However, it requires a manual mapping between the source and target characters where our proposed method can be used for this purpose.

The motion retargeting has also been widely studied in robotics as imitating human demonstrations is unarguably the most natural and non-disruptive form of acquiring robot skills [10]. It can roughly be categorized into two groups: a joint space formulation and a task (Cartesian) space formulations based on the information transferred to the robot.

The joint space retargeting methods transfer the source motions by designing the mapping between joint angles of a source MoCap skeleton and a target robot hardware. [1], [11] studied the retargeting problem by finding the mapping between the joints angles of the source MoCap skeleton and the target robot considering hardware constraints such as handling singularities near gimbal lock and maximum joint velocity using a Sarcos humanoid robot. The MoCap motions are constrained manually to match the degree of freedom (DOF) of the Sarcos and computed by solving IK on individual limbs. [12], [13] further extends the retargeting to whole body control by simultaneously keeping the balance and tracking MoCap data. Recently, Penco et al. presented a real-time motion retargeting method [2] by designing a manual mapping between the joint angles of a Xsens mocap system and the iCub humanoid robot.

On the other hand, the task space formulations utilizes the reference targets in the task space, e.g., hands and elbows. A marker-less retargeting approach was presented in [14] using the Honda humanoid robot, ASIMO. The Cartesian positions of waist, shoulders, elbows, wrists, and head obtained from a depth image are used to control the humanoid by solving IK. It is further extended in [15], [16] to whole body humanoid control. Sit-to-Stand Task using a humanoid robot is studied in [17]. A kinodynamically consistent retargeting method with a set of task points was proposed in [18] which incorporates a dynamically consistent redundancy resolution approach to minimize costly joint motions. Motion retargeting with a multi-contact scenario was studied in [19] with a QP formulation.

Recently, some approaches [10], [20], [21] proposed an optimization-based motion retarget methods. Stochastic Optimization of the Embodiment Mapping (ISOEMP) was proposed in [10] which employs learning-based motion retargeting by optimizing both shape and location of the reference trajectories minimizing a certain cost. While the overall concept of using an optimization method for motion retargeting is similar to ours, ISOEMP focused on motion skills such as transferring a golf swing motion to a 7 DoF robot arm whereas we focus on more expressive motions with both hands such as *salute* or *yawn*. Moreover, ISOEMP only considers transferring a single target trajectory in a task space using an affine transformation. Wang et al. optimized a parametrized skeleton [20] for motion retargeting similar to ours. However, it only focused on a single instance from a depth image using Microsoft Kinect V2 rather than a motion trajectory in a task space. Recent work in [21] simultaneously optimized the geometric mapping between the human model and a robot from the key points in a task space where balancing is also considered using the ZMP constraints. Generating character-like walking motions had been studied in [22] using trajectory optimization.

Measuring the quality of motion retargeting was studied in [23] where a measure for human-like motions was presented using spatiotemporal correspondence. While we do not incorporate such measures, it can further be used to combine with the optimization by simply augmenting the measure to the cost function. The notion of *style* is proposed in [24] where it is defined as a person-specific differences in motions. Okamoto et al. introduced a framework that can generate motions while reflecting specific styles in a ring toss task. While [24] manually designed the motion style features, automatic extraction and stylization of person-specific styles in motion retargeting is a valuable research direction in human-robot interactions (HRIs).

III. Preliminaries

In this section, we present a gradient-free optimization method that is used for the proposed motion retargeting method: coordinate descent Bayesian optimization which gracefully mixes both global and local optimization methods.

A. Coordinate Descent Bayesian Optimization

Bayesian optimization (BO) is a global optimization method that does not require computing the gradient of a cost function [25]. Due to its gradient-free nature, it has been widely used not only for tuning hyperparameters of classifiers [25] but also for robotics domains such as gait optimization [26]. Recently, [27] combined Bayesian optimization with stochastic coordinate descent and proposed coordinate descent Bayesian optimization (CDBO) to optimize the navigation policy for a track race. In this paper, we also use CDBO for optimizing the motion transfer mapping in that we observe that CDBO is more sample-efficient than naive BO in high-dimensional spaces with respect to fine-tuning the details.

Let us first briefly explain the underlying BO method. The goal of BO is to find the minimum of a cost function $f(\boldsymbol{\theta})$ on a compact set Θ where the core philosophy is to model $f(\boldsymbol{\theta})$ using previous observations with a Gaussian process (GP) prior. BO is effective when $f(\cdot)$ is not differentiable

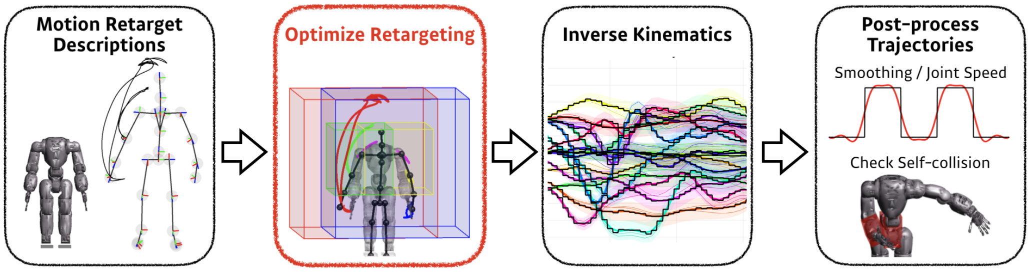

Fig. 1: Overall pipeline of the proposed motion retarget optimization method.

with respect to $\boldsymbol{\theta}$ and the evaluation of $f(\boldsymbol{\theta})$ is expensive to perform such as training and evaluating a model [25]. In this paper, evaluating the cost $f(\boldsymbol{\theta})$ corresponds to computing the cost of motion retarget which is accompanied by running multiple forward kinematics (FKs) of the kinematic model of a robot. More details are explained in Section IV.

In particular, we use Bayesian optimization with expected improvement criteria (BO-EIC) where BO-EIC has shown to outperform well-known GP upper confidence bounds (GP-UCB) on some tasks [25]. More importantly, unlike GP-UCB, it does not require tuning the exploration and exploration tradeoffs. BO-EIC uses the following acquisition function:

$$a(\boldsymbol{\theta}) = \sigma(\boldsymbol{\theta})\left(\gamma(\boldsymbol{\theta})\Phi(\gamma(\boldsymbol{\theta}) + \mathcal{N}(\gamma(\boldsymbol{\theta}); 0, 1)\right) \tag{1}$$

where

$$\gamma(\boldsymbol{\theta}) = \frac{f(\boldsymbol{\theta}_{\text{best}}) - \mu(\boldsymbol{\theta})}{\sigma(\boldsymbol{\theta})}, \tag{2}$$

$\Phi(\cdot)$ is the normal cumulative distribution function, $\boldsymbol{\theta}_{\text{best}}$ is the current best value, and $\mu(\boldsymbol{\theta})$ and $\sigma^2(\boldsymbol{\theta})$ are predictive mean and variance of a GP (interested reader are referred to [28]). We use the following ARD Mateŕn $5/2$ kernel function:

$$K_{\text{M51}}(\boldsymbol{\theta}, \boldsymbol{\theta'}) = \left(1 + \sqrt{5r^2(\boldsymbol{\theta}, \boldsymbol{\theta'})}\right) \exp\left\{-\sqrt{5r^2(\boldsymbol{\theta}, \boldsymbol{\theta'})}\right\} \tag{3}$$

where $r^2(\boldsymbol{\theta}, \boldsymbol{\theta}') = \sum_{d=1}^{D}(\boldsymbol{\theta}_d - \boldsymbol{\theta}'_d)^2 / l_d^2$ which results in twice-differentiable sample functions, an assumption corresponds to quasi-Newton methods, but not unrealistically smooth, such as the widely-used squared exponential kernel.

IV. Proposed Method

In this section, we present an efficient motion retargeting pipeline based on optimizing the mapping between the source 3-D motion data and the target humanoid robot. The proposed method consists of four steps: preparation of motion retargeting, optimizing the motion transfer, computing joint trajectories using iterative IK, and post-processing the joint trajectories. The overall process of the proposed method is shown in Figure 1.

A. *Motion Retarget Descriptions*

The main motivation of this paper is the necessity of an efficient generation of expressive high-quality robot movements from motion datasets. The cornerstone of our motion retargeting method is to define the motion retargeting by transferring the joints of interest (JOI) of a source motion skeleton to the target robot hardware. We would like to emphasize that, apart from parsing source motions and robot morphologies, the only manual process of our method is to define the JOI of both source skeleton and target robot which greatly removes tedious manual processes.

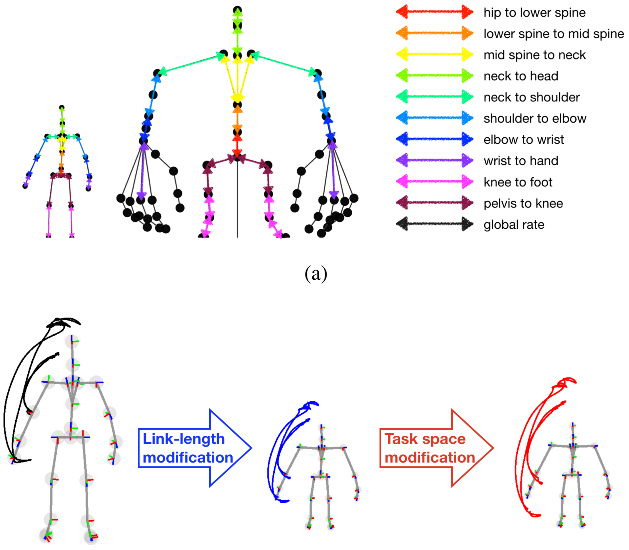

(a)

(b)

Fig. 2: (a) Link length modification parameterizations of human and animation character skeletons. (b) Two-staged transfer of the motion data: link length modification followed by task space modification.

In this work, we define JOI as both hands, elbows, and head for both skeletons and robots inspired by marionette puppeteering. We further show that the whole upper body motions including torso and waist movements can successfully be transferred to the target robot hardware with current JOI configurations in the experiment section.

We assume that we are given a sequence of joints position of a skeleton in the task (Cartesian) space. Given a sequence of joint positions and the topology of the skeleton, we first initialize the kinematic chain of the skeleton with a rigid-body assumption, i.e., compute the Euler angles between joints. The main reason for this is that we will transfer the positions of JOI by modifying the link length of the source skeleton (see Section IV-B for details).

As one cannot fully determine the Euler angles (roll, pitch, and yaw) between two joint positions in the task space, we compute roll and pitch angles between two consecutive joints to remove the ambiguity. Let R and $\mathbf{v}$ be the rotation matrix of a local coordinate and a relative vector from a parent to a child, then a roll angle ϕ and a pitch angle θ are computed as follows:

$$\begin{aligned} \mathbf{v}' &= R^T \mathbf{v} \\ \mathbf{v}' &= \mathbf{v}' / \|\mathbf{v}'\|_2 \\ \phi &= \arcsin\left(-\mathbf{v}'(2)\right), \quad \theta = \operatorname{atan2}\left(\mathbf{v}'(1), \mathbf{v}'(3)\right) \end{aligned} \tag{4}$$

Furthermore, we also compute the joint workspaces of the robot. Here, we compute the Cartesian workspaces of both hands and elbows as shown in Figure 4. Note that this process of computing the workspaces of JOI can be done automatically once the kinematic structure of the robot is successfully parsed from the robot descriptions such as from the unified robot description format (URDF).

B. Optimize Retargeting

Once we have the JOI of both source skeleton and target robot, we automatically optimize the adequate transfer between two sets of JOI using the coordinate descent Bayesian optimization (CDBO) in Section III-A. To this end, we define two main components for the optimization. One is the parametrization of the motion transfer and the other is the cost function for assessing the quality of the transfer.

Let us first introduce the motion transfer parametrization. The motion transfer of the source motions is done with two steps: link length adjustments of the base skeleton and task space modifications of the resulting trajectories of JOI.

Suppose that we are given a base skeleton[1] and a sequence of roll and pitch angles of the motion computed from (4). Then, the link length modification is done with 11 parameters: global rate, hip to lower spine, lower spine to mid spine, mid spine to neck, neck to head, neck to shoulder, shoulder to elbow, elbow to wrist, wrist to hand, knee to foot, and pelvis to knee as shown in Figure 2(a). Once we have the normalized (link-length adjusted) skeleton and a sequence of roll and pitch angles of each joint, task-space trajectories of JOI is computed using FK.

The adjusted JOI trajectories are further fine-tuned in the task space with six parameters: three parameters for scaling and three parameters for translation in the Cartesian space, respectively, where both scaling and translation are done with respect to the shoulder position. The link length modification and task space modification of right hand and elbow trajectories are illustrated in Figure 2(b).

As we cast the motion retargeting problem as an optimization problem, we also need a measure for assessing the quality of the motion transfer. We carefully design the cost function composed of four different components. Suppose we are given adjusted trajectories of JOI in the task space and the target humanoid robot at its homing position.

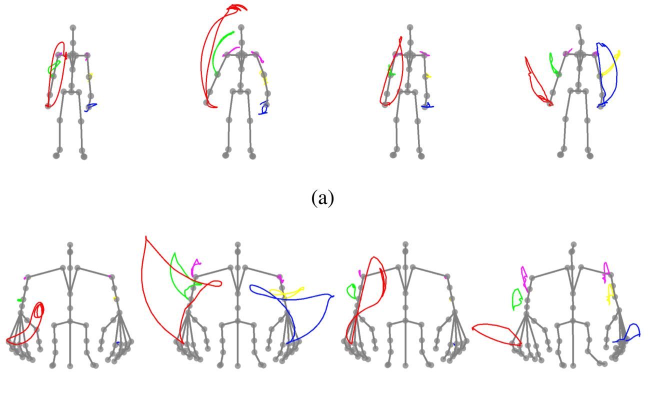

Fig. 3: Two 3D motion datasets acquired from (a) a human demonstrator performing (*big point*, *big wave*, *salute*, and *yawn*) and (b) an animation character, *Bork*, performing (*go on*, *this big*, *greeting*, and *tada*).

1) **Location cost** c_{loc}: Task space position differences between the initial position of the both right and left adjusted shoulder positions and the corresponding shoulder positions of the target humanoid.
2) **Link length cost** c_{link}: Link length differences of both right and left shoulder to elbow limbs and elbow to hand limbs between the adjusted source skeleton and the target humanoid.
3) **Workspace cost** c_{ws}: Maximum distance from the task space trajectories of JOI and corresponding workspaces.
4) **Trajectory cost** c_{traj}: The differences between the normalized trajectories of JOI of both raw motion data and the adjusted motion data. The normalization is done by centering the trajectories with respect to each axis and scale the centered trajectories so that all trajectories lie within -1 and $+1$.

Each cost is further divided by the height of the target humanoid and the weighted sum of costs are used for the optimization:

$$c_{\text{total}} = (w_{\text{loc}} c_{\text{loc}} + w_{\text{link}} c_{\text{link}} + w_{\text{ws}} c_{\text{ws}} + w_{\text{traj}} c_{\text{traj}}) / h_{\text{robot}}$$

where $w_{\text{loc}} = 100$, $w_{\text{link}} = 100$, $w_{\text{ws}} = 100$, $w_{\text{traj}} = 10$, and h_{robot} is the height of the robot.

C. Compute Joint Trajectories with IKs

Once the JOI trajectories in the task space are computed, joint trajectories are computed via an iterative IK method using an augmented Jacobian method to incorporate multiple target joints. At each iteration, we add a simple heuristic to recover its initial state to overcome singularities. The resulting joint trajectories are further smoothed using a Gaussian random path [29].

Both self-collision and joint limit constraints are handled while solving IK. To check self-collision, we first find the

[1] We simply use the initial skeleton at $t = 0$ in the 3-D motion dataset.

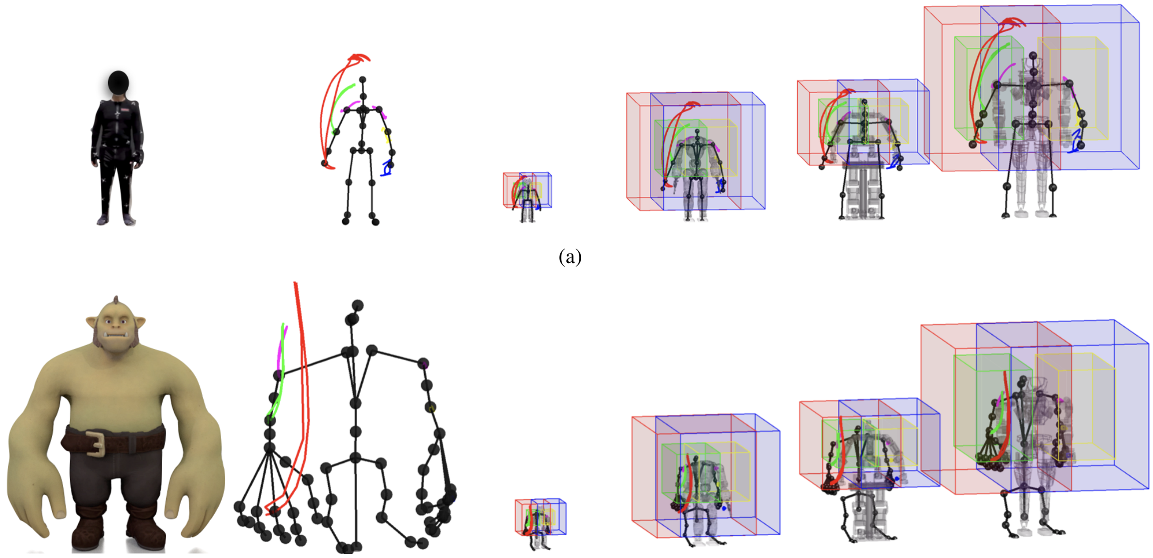

(a)

(b)

Fig. 4: Motion retarget results using 3-D motion data from (a) a human doing a *big wave* motion and (b) an animation character doing a pointing action. The trajectories of right hand, right elbow, right shoulder, left hand, left elbow, and left shoulder are shown with red, green, purple, blue, yellow, and purple, respectively. The workspaces of both hands and elbows are shown with corresponding colors, respectively.

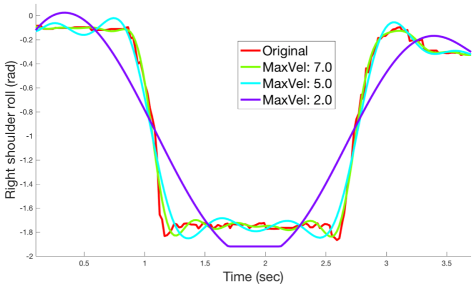

Fig. 5: Joint trajectories of right shoulder roll joint of COMAN with different maximum velocity limits. when performing the *big wave* motion.

bounding cubes of links from the CAD files and compute the collision using the GJK algorithm [30]. Suppose $\mathbf{q}$ be current joint angles and $d\mathbf{q}$ be the angle difference from the augmented Jacobian method. If self-collision is expected to occur at the next time step, i.e., $\mathbf{q}+d\mathbf{q}$ occurs self-collision, we first find the revolute-joint index that does not lead to self-collision when updating $\delta\mathbf{q}(i)$ where i is the joint index. If multiple joints are found, we simply update the one whose $|\delta\mathbf{q}(i)|$ is the biggest, and otherwise, do not update the angles and proceed to the next target JOI.

To handle the joint position limits, we first find the joint indices of $\mathbf{q}+d\mathbf{q}$ that exceed the joint limits with some small margin, and re-run IK excluding the corresponding joints. We found this simple heuristics works remarkably well on handing joint limit constraints compared to virtual force based methods [14].

D. *Post-process Joint Trajectories*

The resulting joint trajectory from IK may not be runnable to a robot due to physical constraints such as joint velocity constraints. As the smoothness of the resulting trajectory varies based on the hyperparameters of a kernel function, we simply increase the length parameter of a rational quadratic kernel (RQ) until the resulting trajectory satisfies the velocity constraints where the velocities are computed with finite-differences. Figure 5 illustrates post-processed joint trajectories of right should roll joint of COMAN with different maximum velocity limits. when performing the *big wave* motion. However, one can analytically compute the gradient of a trajectory when using a GRP.

E. *Remark*

We would like to emphasize that the proposed motion retargeting method only requires the JOI descriptions of the source motion and the humanoid robot. The link length modification shown in Figure 2(a) is straightforward to compute using the JOI of the robot. Due to this simplicity, we evaluate the performance of the proposed method on every combination of four different humanoid robots and two different types of motion data from both a human demonstrator and an animation character.

V. Experiments

To show that our method can effectively be applied to diverse motion datasets and humanoid robots, we use 36 different motions from two 3D motion datasets, 4 motions (*big point*, *big wave*, *salute*, and *yawn*) from three human demonstrators and 4 motions (*go on*, *this big*, *greeting*,

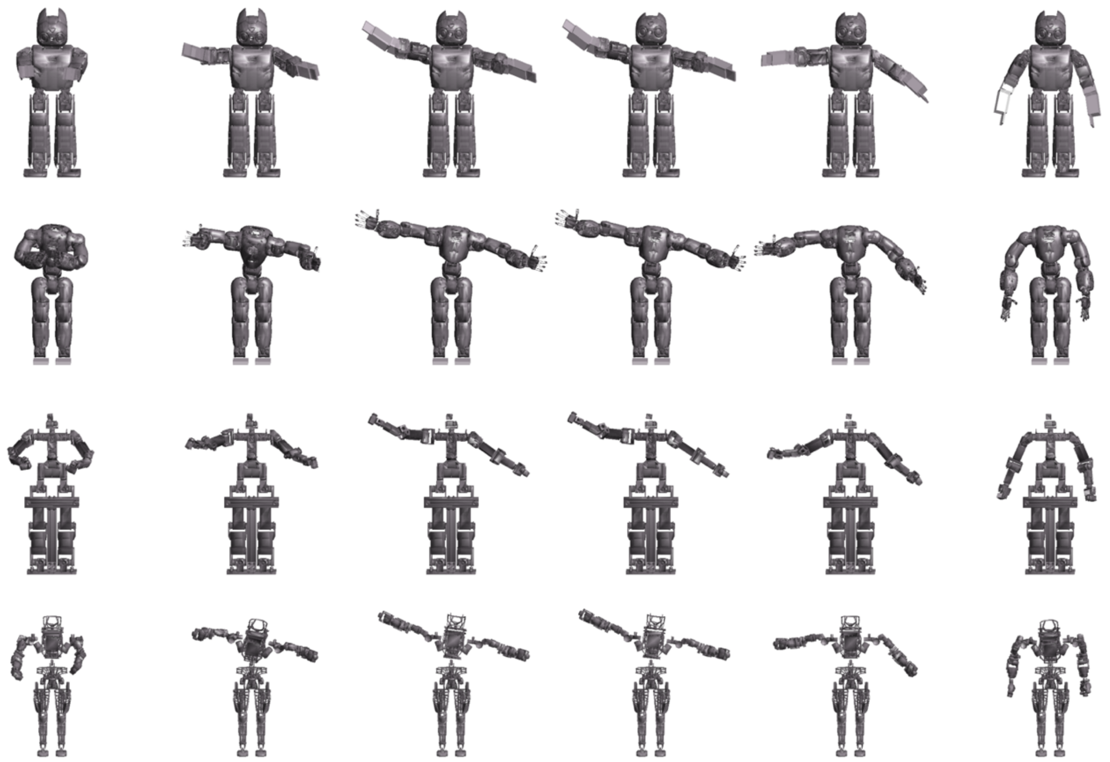

Fig. 6: Snapshots of four different robots performing the *this big* motion of *Bork*.

and *tada*) from an animation character, *Bork*, as shown in Figure 3 and four different humanoid robots: DARwIn-OP, COMAN, THORMANG, and Atlas whose sizes and morphologies vary significantly as shown in Figure 4.

A. Motion Retarget Results

The motion retargeting results of the proposed method using a *big wave* motion from a human demonstrator and a *greeting* motions from *Bork* are shown in Figure 4. The workspaces of right hand, right elbow, left hand, and left elbow are shown with red, greed, blue, and yellow cubes, respectively. Note that these workspaces of a robot are computed automatically once we parsed to robot descriptions.

We can see that the shoulder positions of the adjusted skeletons match those of the corresponding humanoid robots. Note that The adjusted skeleton of THORMANG for the *big wave* motions shown in Figure 4(a) has short upper-body length and the shoulder positions are little lower than those of THORMANG. This is because the workspaces of both hands of THORMANG are relatively small in height due to the joint limit constraints and having a short upper-body makes the resulting JOI trajectories in the task space fitted in the corresponding JOI workspaces. The snapshots of four humanoid robots performing the *this big* motion are illustrated in Figure 6

B. Ablation Study of different Joints of Interest

Here, we show how different JOI affect the resulting motions using COMAN with a *Bork*'s *this big* motion. We believe COMAN is suitable for this purpose in that it has human-like hands. In particular, we use three different JOI configurations: 1) hand positions, 2) hand and elbow positions, and 3) hand positions, hand rotations, and elbow positions and the resulting motion of COMAN performing *this big* motion of *Bork* are shown in Figure 7.

C. Using Physical Humanoid Robots

The snapshots of COMAN and THORMANG doing the *big point* motion are shown in Figure 8. Since the lower body of THORMANG in our configuration is tied with a fixed frame, we did not care about the balancing. For balancing COMAN, the lower body joints are controlled with the stabilization method proposed in [31]. It is worthwhile noting that, while we only use four JOI of both hands and elbows, the waist movement of the human demonstrator is successfully transferred to COMAN.

VI. Conclusion

In this paper, we have presented the motion retargeting pipeline for generating expressive robot movements. To this end, we proposed an optimization-based motion transfer method utilizing both link length modifications of a base skeleton and task space fine-tuning. The only manual process is to define the joints of interest (JOI) of both source skeleton

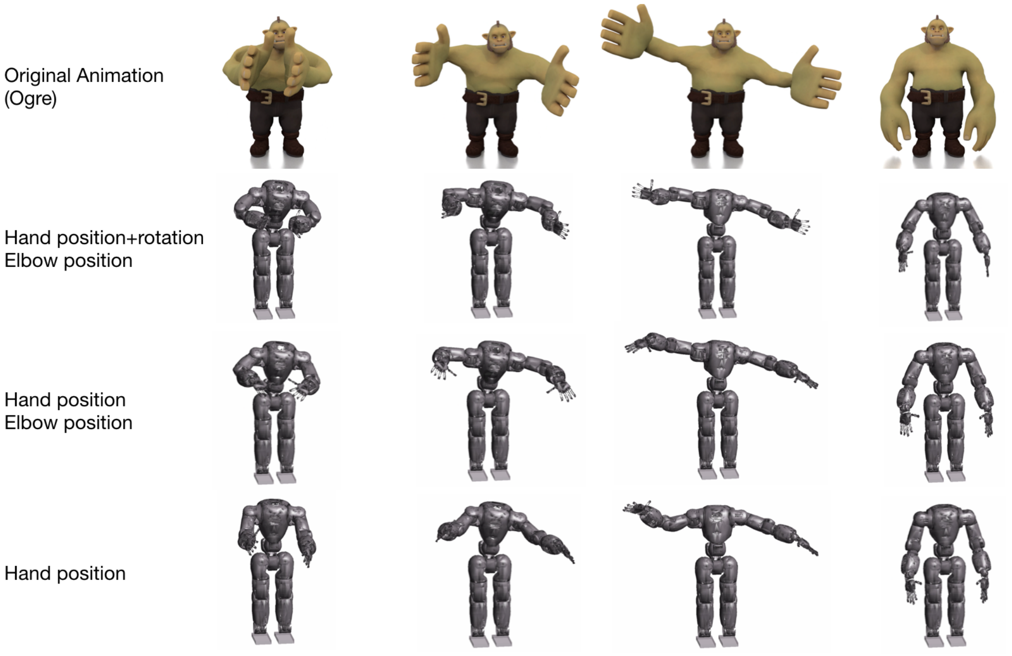

Fig. 7: COMAN motions performing *Bork*'s *this big* motion with different joints of interest.

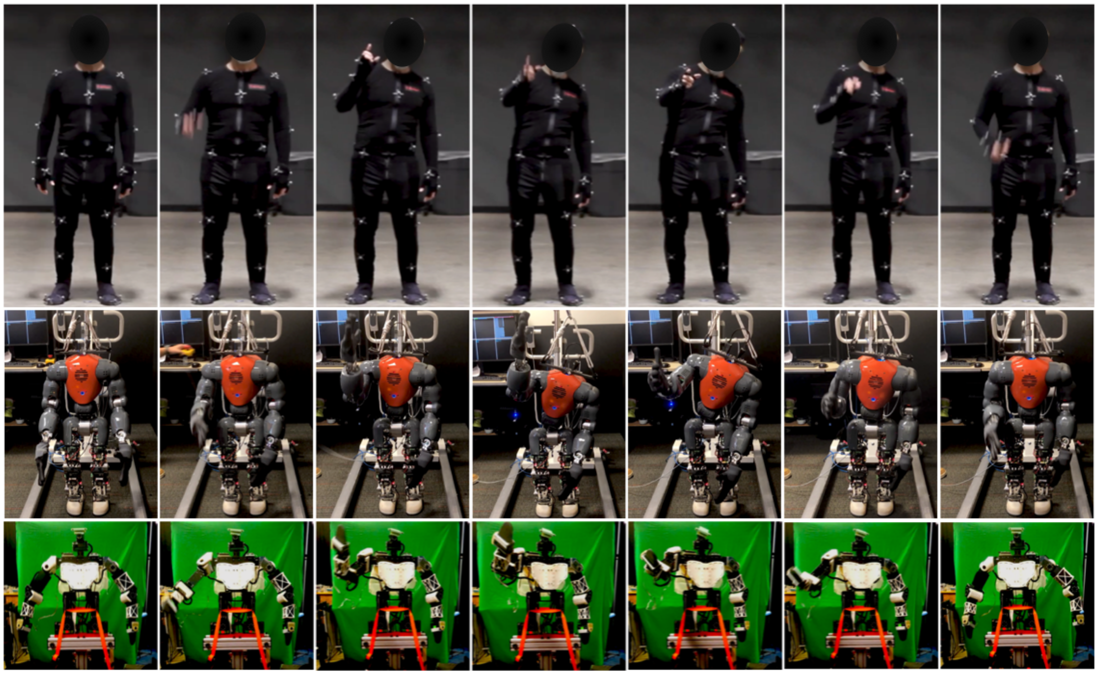

Fig. 8: From top to bottom rows, the *big point* motion performed by a human demonstrator, COMAN, and THORMANG.

and target robot which makes the whole pipeline simple and effective.

To evaluate the effectiveness of the motion retarget pipeline, we used two different motion datasets from three human demonstrators and an animation character and transfer the motions to four different humanoid robots: DARwIn-OP, COMAN, THORMANG, and Atlas in simulated environments. We also controlled real physical COMAN and THORMANG to show that the proposed method can actually be deployed to physical robots.

One limitation of our work is that it relies on the manual selection of joints of interests (JOI). We believe that the automatic selection of JOI given the motion data and robot descriptions might be a promising research direction. One could apply a hypergraph matching algorithm [32] for this purpose. Future research could also examine the optimization of the joint trajectories with whole-body stability constraints.

Acknowledgement

We thank Daniel Campos Zamora and Kyna McIntosh for assistance with making an illustrative video.

References

[1] N. S. Pollard, J. K. Hodgins, M. J. Riley, and C. G. Atkeson, "Adapting human motion for the control of a humanoid robot," in *IEEE Proc. of International Conference on Robotics and Automation (ICRA)*, vol. 2. IEEE, 2002, pp. 1390–1397.

[2] L. Peneo, B. Clément, V. Moduano, E. M. Hoffman, G. Nava, D. Pucci, N. G. Tsagarakis, J.-B. Mourert, and S. Ivaldi, "Robust real-time whole-body motion retargeting from human to humanoid," in *Proc. of the IEEE International Conference on Humanoid Robots*. IEEE, 2018, pp. 425–432.

[3] M. Gleicher, "Retargetting motion to new characters," in *Proceedings of the 25th annual conference on Computer graphics and interactive techniques*. ACM, 1998, pp. 33–42.

[4] K. Grochow, S. L. Martin, A. Hertzmann, and Z. Popović, "Style-based inverse kinematics," in *ACM transactions on graphics (TOG)*, vol. 23, no. 3. ACM, 2004, pp. 522–531.

[5] K. Yamane, Y. Ariki, and J. Hodgins, "Animating non-humanoid characters with human motion data," in *Proc. of the ACM SIGGRAPH/Eurographics Symposium on Computer Animation*. Eurographics Association, 2010, pp. 169–178.

[6] C. Hecker, B. Raabe, R. W. Enslow, J. DeWeese, J. Maynard, and K. van Prooijen, "Real-time motion retargeting to highly varied user-created morphologies," in *ACM Transactions on Graphics (TOG)*, vol. 27, no. 3. ACM, 2008, p. 27.

[7] N. D. Lawrence, "Gaussian process latent variable models for visualisation of high dimensional data," in *Advances in neural information processing systems*, 2004, pp. 329–336.

[8] K. Yamane and Y. Nakamura, "Natural motion animation through constraining and deconstraining at will," *IEEE Transactions on visualization and computer graphics*, vol. 9, no. 3, pp. 352–360, 2003.

[9] X. B. Peng, P. Abbeel, S. Levine, and M. van de Panne, "Deepmimic: Example-guided deep reinforcement learning of physics-based character skills," *ACM Transactions on Graphics (TOG)*, vol. 37, no. 4, p. 143, 2018.

[10] G. Maeda, M. Ewerton, D. Koert, and J. Peters, "Acquiring and generalizing the embodiment mapping from human observations to robot skills," *IEEE Robotics and Automation Letters*, vol. 1, no. 2, pp. 784–791, 2016.

[11] A. Safonova, N. Pollard, and J. K. Hodgins, "Optimizing human motion for the control of a humanoid robot," *Proc. Applied Mathematics and Applications of Mathematics*, vol. 78, 2003.

[12] K. Yamane and J. Hodgins, "Simultaneous tracking and balancing of humanoid robots for imitating human motion capture data," in *IEEE/RSJ International Conference on Intelligent Robots and Systems (IROS)*. IEEE, 2009, pp. 2510–2517.

[13] K. Yamane, S. O. Anderson, and J. K. Hodgins, "Controlling humanoid robots with human motion data: Experimental validation," in *IEEE-RAS International Conference on Humanoid Robots (Humanoids)*. IEEE, 2010, pp. 504–510.

[14] B. Dariush, M. Gienger, A. Arumbakkam, C. Goerick, Y. Zhu, and K. Fujimura, "Online and markerless motion retargeting with kinematic constraints," in *IEEE/RSJ International Conference on Intelligent Robots and Systems (IROS)*, 2008.

[15] B. Dariush, M. Gienger, B. Jian, C. Goerick, and K. Fujimura, "Whole body humanoid control from human motion descriptors," in *Proc. of International Conference on Robotics and Automation (ICRA)*. IEEE, 2008, pp. 2677–2684.

[16] B. Dariush, M. Gienger, A. Arumbakkam, Y. Zhu, B. Jian, K. Fujimura, and C. Goerick, "Online transfer of human motion to humanoids," *International Journal of Humanoid Robotics*, vol. 6, no. 02, pp. 265–289, 2009.

[17] M. Mistry, A. Murai, K. Yamane, and J. Hodgins, "Sit-to-stand task on a humanoid robot from human demonstration," in *IEEE-RAS International Conference on Humanoid Robots (Humanoids)*. IEEE, 2010, pp. 218–223.

[18] G. Bin Hammam, P. M. Wensing, B. Dariush, and D. E. Orin, "Kinodynamically consistent motion retargeting for humanoids," *International Journal of Humanoid Robotics*, vol. 12, no. 04, p. 1550017, 2015.

[19] K. Otani and K. Bouyarmane, "Adaptive whole-body manipulation in human-to-humanoid multi-contact motion retargeting," in *IEEE-RAS International Conference on Humanoid Robots (Humanoids)*. IEEE, 2017, pp. 446–453.

[20] S. Wang, X. Zuo, R. Wang, F. Cheng, and R. Yang, "A generative human-robot motion retargeting approach using a single depth sensor," in *Proc. of International Conference on Robotics and Automation (ICRA)*. IEEE, 2017, pp. 5369–5376.

[21] K. Ayusawa and E. Yoshida, "Motion retargeting for humanoid robots based on simultaneous morphing parameter identification and motion optimization," *IEEE Transactions on Robotics*, vol. 33, no. 6, pp. 1343–1357, 2017.

[22] S. Song, J. Kim, and K. Yamane, "Development of a bipedal robot that walks like an animation character," in *Proc. of International Conference on Robotics and Automation (ICRA)*. IEEE, 2015, pp. 3596–3602.

[23] M. J. Gielniak and A. L. Thomaz, "Spatiotemporal correspondence as a metric for human-like robot motion," in *Proc. of the International conference on Human-robot interaction*. ACM, 2011, pp. 77–84.

[24] T. Okamoto, T. Shiratori, M. Glisson, K. Yamane, S. Kudoh, and K. Ikeuchi, "Extraction of person-specific motion style based on a task model and imitation by humanoid robot," in *IEEE/RSJ International Conference on Intelligent Robots and Systems (IROS)*. IEEE, 2014, pp. 1347–1354.

[25] J. Snoek, H. Larochelle, and R. P. Adams, "Practical Bayesian optimization of machine learning algorithms," in *Advances in neural information processing systems*, 2012, pp. 2951–2959.

[26] R. Calandra, A. Seyfarth, J. Peters, and M. P. Deisenroth, "An experimental comparison of bayesian optimization for bipedal locomotion," in *Proc. of the IEEE International Conference on Robotics and Automation (ICRA)*. IEEE, 2014, pp. 1951–1958.

[27] R. Oliveira, F. H. Rocha, L. Ott, V. Guizilini, F. Ramos, and V. Grassi, "Learning to race through coordinate descent bayesian optimisation," in *Proc. of the IEEE International Conference on Robotics and Automation (ICRA)*. IEEE, 2018, pp. 6431–6438.

[28] C. E. Rasmussen, "Gaussian processes for machine learning," 2006.

[29] S. Choi, K. Lee, and S. Oh, "Gaussian random paths for real-time motion planning," in *Proc. of the International Conference on Intelligent Robots and Systems*. IEEE, 2016, pp. 1456–1461.

[30] G. v. d. Bergen, "A fast and robust gjk implementation for collision detection of convex objects," *Journal of graphics tools*, vol. 4, no. 2, pp. 7–25, 1999.

[31] Z. Li, B. Vanderborght, N. G. Tsagarakis, L. Colasanto, and D. G. Caldwell, "Stabilization for the compliant humanoid robot coman exploiting intrinsic and controlled compliance," in *Proc. of the IEEE International Conference of Robotics and Automation (ICRA)*. IEEE, 2012, pp. 2000–2006.

[32] H. Jin Chang, T. Fischer, M. Petit, M. Zambelli, and Y. Demiris, "Kinematic structure correspondences via hypergraph matching," in *Proc. of the IEEE Conference on Computer Vision and Pattern Recognition*, 2016, pp. 4216–4225.